Gata4 potentiates second heart field proliferation and Hedgehog signaling for cardiac septation

Lun Zhou[a,b,1], Jielin Liu[c,1], Menglan Xiang[a], Patrick Olson[a], Alexander Guzzetta[d,e,f], Ke Zhang[g,h], Ivan P. Moskowitz[d,e,f,2,3], and Linglin Xie[a,c,2,3]

[a]Department of Basic Sciences, University of North Dakota, Grand Forks, ND 58202; [b]Department of Gerontology, Tongji Hospital, Huazhong University of Science and Technology, Wuhan, Hubei, 430030, China; [c]Department of Nutrition and Food Sciences, Texas A&M University, College Station, TX 77843; [d]Department of Pediatrics, The University of Chicago, Chicago, IL 60637; [e]Department of Pathology, The University of Chicago, Chicago, IL 60637; [f]Department of Human Genetics, The University of Chicago, Chicago, IL 60637; [g]Department of Pathology, University of North Dakota, Grand Forks, ND 58202; and [h]North Dakota Idea Network of Biomedical Research Excellence Bioinformatics Core; University of North Dakota, Grand Forks ND 58202

Edited by Eric N. Olson, University of Texas Southwestern Medical Center, Dallas, TX, and approved January 13, 2017 (received for review March 29, 2016)

***GATA4*, an essential cardiogenic transcription factor, provides a model for dominant transcription factor mutations in human disease. Dominant GATA4 mutations cause congenital heart disease (CHD), specifically atrial and atrioventricular septal defects (ASDs and AVSDs). We found that second heart field (SHF)-specific *Gata4* heterozygote embryos recapitulated the AVSDs observed in germline *Gata4* heterozygote embryos. A proliferation defect of SHF atrial septum progenitors and hypoplasia of the dorsal mesenchymal protrusion, rather than anlage of the atrioventricular septum, were observed in this model. Knockdown of the cell-cycle repressor phosphatase and tensin homolog (*Pten*) restored cell-cycle progression and rescued the AVSDs. *Gata4* mutants also demonstrated Hedgehog (Hh) signaling defects. Gata4 acts directly upstream of *Hh* components: Gata4 activated a *cis*-regulatory element at *Gli1* in vitro and occupied the element in vivo. Remarkably, SHF-specific constitutive Hh signaling activation rescued AVSDs in Gata4 SHF-specific heterozygous knockout embryos. Pten expression was unchanged in *Smoothened* mutants, and Hh pathway genes were unchanged in *Pten* mutants, suggesting pathway independence. Thus, both the cell-cycle and Hh-signaling defects caused by dominant *Gata4* mutations were required for CHD pathogenesis, suggesting a combinatorial model of disease causation by transcription factor haploinsufficiency.**

Gata4 | ASDs | Hedgehog signaling | second heart field | cell cycle

Gata4, a member of the GATA family of zinc finger transcription factors, is an essential cardiogenic transcriptional regulator implicated in many aspects of cardiac development and function (1–15). Human genetic studies have implicated dominant GATA4 mutations in atrial septal defects (ASDs), including atrioventricular (AV) septal defects (AVSDs), in human individuals and families (2, 16–21). Gata4 is a transcriptional activator of genes essential for cardiac function. Although important Gata4 transcriptional targets in the heart have been identified, such as *Nppa*, *α-MHC*, *α-CA*, B-type natriuretic peptide (*BNP*), *Mef2c*, and *Cyclin D2* (1, 7, 22), none has been linked to cardiac structural defects. Therefore, the Gata4-driven regulatory networks that are essential for atrial septation remain unknown.

The developmental ontogeny of ASDs has undergone recent revision. ASD is a broad designation for congenital heart disease (CHD) including multiple distinct anatomic defects of the atrial septum. Development of the atrial septum includes contributions from distinct lineages including the AV endocardial cushions, the primary atrial septum (PAS), and the dorsal mesenchymal protrusion (DMP) (23–29). Deficiency of the DMP results in primum ASD, a type of AVSD. Recent work has demonstrated that atrial septation is dependent on the second heart field (SHF), a group of cardiac progenitors that make late additions to the heart (24, 29–32). For example, genetic inducible fate mapping (GIFM) has shown that the entire atrial septum, including the DMP, derives from the SHF (32). Furthermore, the molecular requirement for the Hedgehog (Hh) and *BMP* signaling pathways and the *Tbx5* cardiogenic transcription factor for AV septation reside in the SHF (32–38). These observations lay the groundwork for investigating the molecular pathways required for atrial septum formation in SHF cardiac progenitor cells.

We investigated the lineage-specific requirement for *Gata4* in atrial septation and found that SHF-specific heterozygote *Gata4* knockout recapitulated the AVSDs observed in germline heterozygote *Gata4* knockouts in mice. *Gata4* deletion in the SHF caused a failure of DMP formation and cell-cycle progression defects that were consistent with disrupted *Cdk4*/*Cyclin D2* expression. AVSDs caused by heterozygous SHF *Gata4* knockout could be rescued by knockdown of the cell-cycle repressor phosphatase and tensin homolog (*Pten*), which restored expression of *Cdk4* and cell-cycle progression. Heterozygous Gata4 deletion also caused SHF Hh signaling defects. Hh signaling markers were diminished in SHF-specific *Gata4* heterozygous embryos, and *Gata4* interacted with the obligate Hh receptor gene Smoothened (*Smo*) in vivo. A Gata4-driven enhancer was identified at *Gli1*, a modulator and target of Hh signaling. Furthermore, AVSDs caused by SHF-specific *Gata4* heterozygosity were rescued by constitutive activation of Hh signaling in the SHF. These observations define two independent pathways disrupted by heterozygous *Gata4* knockout. Restoration of either pathway rescues atrial septation in Gata4 heterozygous embryos, suggesting that disruption of both pathways is required for ASD pathogenesis in this model of dominant transcription factor mutation.

Significance

Dominant GATA4 mutations cause congenital heart defects in humans, but the mechanistic basis whereby Gata4 haploinsufficiency causes disease is unknown. We demonstrate that Gata4 is required in a subset of cardiac progenitor cells called the "second heart field" for cardiac septation. Furthermore, we identified two distinct pathways downstream of *Gata4*, phosphatase and tensin homolog (*Pten*)-modulated cell-cycle transition and Hedgehog signaling, which appear to act independently. Restoration of either *Pten*-mediated cell-cycle transition or Hedgehog signaling restored cardiac septation in *Gata4*-mutant mice, suggesting that defects in both pathways are required for disease causation. This work generates a working model for understanding the molecular basis of human congenital heart disease caused by dominant transcription factor mutations.

Author contributions: L.Z., J.L., M.X., P.O., A.G., and L.X. performed research; K.Z. and L.X. analyzed data; I.P.M. and L.X. designed research; and I.P.M. and L.X. wrote the paper.

The authors declare no conflict of interest.

This article is a PNAS Direct Submission.

[1]L.Z. and J.L. contributed equally to this work.

[2]I.P.M. and L.X. contributed equally to this work.

[3]To whom correspondence may be addressed. Email: linglin.xie@tamu.edu or imoskowitz@uchicago.edu.

This article contains supporting information online at www.pnas.org/lookup/suppl/doi:10.1073/pnas.1605137114/-/DCSupplemental.

Results

Previous work has demonstrated *Gata4* expression in the heart, including the dorsal mesocardium, myocardium, and endocardium, during AV septation (1, 3, 8, 39–42). *Gata4* is also expressed in the SHF of human embryos from Carnegie stage 10–16 (39, 43). We examined Gata4 protein expression in embryonic day (E)9.5 wild-type mouse embryos by immunohistochemistry (IHC) staining. As expected, strong Gata4 expression was observed in the heart, including the atrium, ventricles, and outflow tract (Fig. 1*A*). Strong Gata4 expression also was observed in the dorsal mesocardium and SHF mesenchyme behind the heart (Fig. 1*A*, B). The density of Gata4-expressing cells appeared to be higher in the posterior SHF (pSHF) than in the anterior SHF (aSHF) (Fig. 1*B*). These observations were confirmed by *Gata4* transcript levels analyzed by RNA-sequencing (RNA-seq) from aSHF, pSHF, and heart, each microdissected from wild-type mouse embryos at E9.5 (Table 1) (44). *Gata4* expression, represented by fragments per kilobase of transcript per million mapped reads (FPKM) values, was high in the heart (37.43 ± 6.31) and the pSHF (18.86 ± 4.09) and was lower in the aSHF (4.00 ± 3.12) (Table 1). Expression of the control SHF marker genes *Fgf8*, *Isl1*, *Tbx1*, and *Gli1* was substantially higher in the SHF than in the heart (Table 1). Furthermore, FPKM counts for *Tbx5* were greatly enriched in the heart and pSHF as compared to the aSHF in accordance with historical in situ hybridization experiments (35, 43, 45–47). These results indicated strong Gata4 expression in the pSHF.

To determine the lineage requirement for *Gata4* in AV septation, we analyzed mouse embryos with lineage-specific, heterozygous deletion of *Gata4* in the germline, myocardium, endocardium, or SHF. We used a *Gata4* floxed allele with loxP sites flanking the second exon, encoding the first coding exon essential for Gata4 function (8), and converted it into lineage-specific knockouts with a series of murine lineage-specific *Cre* lines. Tissue-specific knockdown of Gata4 was confirmed by gel electrophoresis (Fig. S1). This *Gata4* floxed allele resulted in a 20% reduction in Gata4 protein level before Cre excision (6, 8). We converted a single $Gata4^{fl/+}$ into a germline knockout using $EIIa^{Cre}$ (48). Although $Gata4^{fl/+}$ (n = 13) and $EIIa^{Cre/+}$ (n = 12) embryos demonstrated normal cardiac anatomy, including complete atrial septation at E13.5 (Fig. 1 *C*, *D*, *F*, and *G*), 39% (7/18) of $Gata4^{+/-}$; $EIIa^{Cre/+}$ embryos demonstrated primum ASDs with absence of the DMP ($P = 0.0053$ vs. $Gata4^{fl/+}$ or $EIIa^{Cre/+}$) (Fig. 1 *E* and *H* and Table 2). This observation is consistent with previous reports implicating germline heterozygous *Gata4* deletion in ASDs (6). We examined *Gata4* heterozygosity in the myocardium by combining cardiomyocyte-specific *Tnt:Cre* (49) with $Gata4^{fl/+}$ (Fig. 1 *I* and *N* and Table 2). Normal atrial septation was observed in all $Tnt^{Cre/+}$; $Gata4^{fl/+}$ (12/12) and littermate control $Gata4^{fl/+}$ (13/13) embryos at E13.5 ($P = 1$) (Fig. 1 *J* and *O*). We examined *Gata4* haploinsufficiency in the endocardium by combining endocardial-specific *Tie2:Cre* (34, 50) with $Gata4^{fl/+}$ (Fig. 1 *K* and *P* and Table 2). Normal atrial septation was observed in all $Tie2^{Cre/+}$; $Gata4^{fl/+}$ mutant embryos (23/23) and littermate control $Gata4^{fl/+}$ embryos (13/13) at E13.5 ($P = 1$) (Fig. 1 *I* and *M*). These results demonstrated that *Gata4* haploinsufficiency in the myocardium or endocardium supported normal atrial septation in a mixed genetic background (*Materials and Methods*).

We hypothesized that *Gata4* was required in the SHF for atrial septation (32, 34). We combined $Gli1^{Cre\text{-}ERT2/+}$, expressed in SHF Hh signal-receiving cells, with $Gata4^{fl/+}$ to generate heterozygote SHF-specific *Gata4*-knockout embryos (35). CreERT2 was activated by tamoxifen (TM) administration at E7.5 and E8.5 or at E8.5 and E9.5 in $Gli1^{Cre\text{-}ERT2/+}$;$Gata4^{fl/+}$ embryos, a regime previously used to implicate Hh signaling in the SHF for AV septation (32). Primum ASDs were observed in 62% (13/21) of $Gli1^{Cre\text{-}ERT2/+}$;$Gata4^{fl/+}$ embryos with TM administration at E7.5 and E8.5 but not in littermate control $Gata4^{fl/+}$ embryos (0/15; $P < 0.0001$) or $Gli1^{Cre\text{-}ERT2/+}$ embryos (0/15; $P < 0.0001$) at E13.5 (compare Fig. 1 *I* and *N* with Fig. 1 *L* and *Q* and see Table 1). $Gli1^{Cre\text{-}ERT2/+}$;$Gata4^{fl/+}$ embryos also displayed a double-outlet right ventricle (DORV) with ventricular septal defect (11/18, 83%)

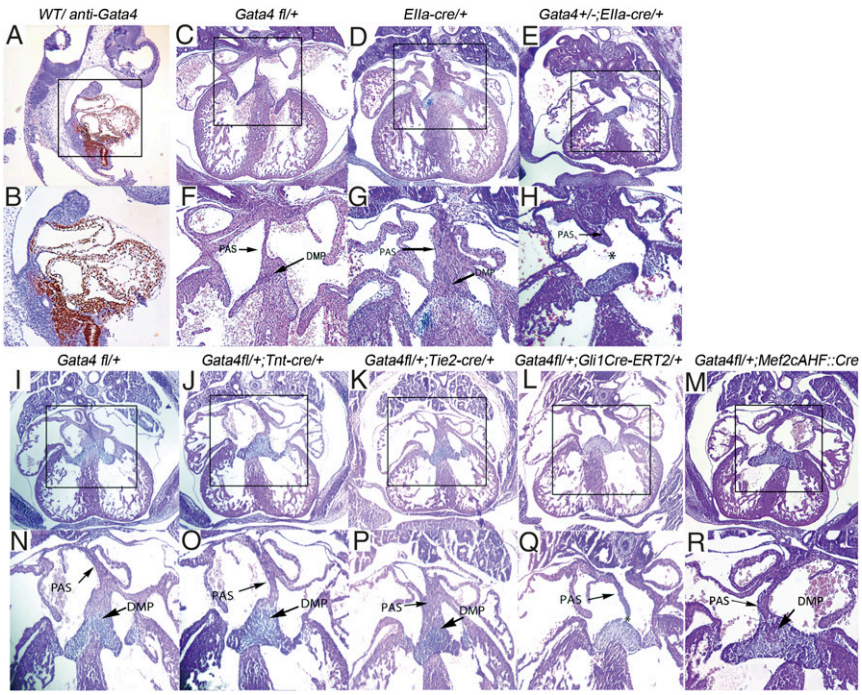

Fig. 1. *Gata4* is required in the atrial septum progenitor of pSHF for atrial septation. (*A* and *B*) IHC staining of Gata4 in wild-type mouse embryos at E9.5. (*C*–*R*) Histology of *Gata4* transgenic mouse embryo hearts at E13.5. Asterisks indicate missing structures of atrial septation. *B*, *F*–*H*, and *N*–*R* show the boxed areas in *A*, *C*–*E*, and *I*–*M*, respectively, at higher magnification. (Magnification: 40× in *A*, *C*–*E*, and *I*–*M*; 100× in *B*, *F*–*H*, and *N*–*R*.)

Table 1. Expression of selected genes in heart, aSHF, and pSHF of mouse embryos at E9.5 measured by RNA-seq (n = 6)

Gene	Heart	aSHF	pSHF
Gata4	37.43 ± 6.31[a]	4.00 ± 3.12[b]	18.86 ± 4.09[c]
Tbx5	24.77 ± 2.21[a]	0.91 ± 0.76[b]	12.28 ± 1.98[c]
Fgf8	2.12 ± 1.16[a]	6.94 ± 2.36[b]	3.87 ± 1.76[b]
Tbx1	0.39 ± 0.17[a]	14.12 ± 1.64[b]	9.20 ± 2.12[c]
Gli1	1.32 ± 0.39[a]	14.76 ± 4.52[b]	16.26 ± 4.26[b]
Isl1	3.71 ± 1.21[a]	22.84 ± 3.78[b]	17.44 ± 4.01[b]
Pten	13.06 ± 0.79[a]	14.92 ± 1.16[a]	14.88 ± 0.70[a]
Adipoq	0.18 ± 0.12[a]	0.00 ± 0.02[a]	0.02 ± 0.04[a]

Mouse embryos were microdissected at E9.5 as described in *Materials and Methods*. The significant difference in the expression of each gene in heart, aSHF, and pSHF was tested by ANOVA analysis. Different letters denote a significant difference between different tissues (a vs. b, a vs. c, b vs. c; $P < 0.05$, $n = 6$). *Adipoq*, adiponectin.

(Fig. S2) and thinner myocardium (Fig. 1 and Fig. S2). Primum ASD in $Gli1^{Cre\text{-}ERT2/+}$;$Gata4^{fl/+}$ embryos administered TM at E8.5 and E9.5 occurred at a much lower frequency (2/9) that was not statistically different from that in littermate control $Gata4^{fl/+}$ embryos (0/10, $P = 0.0675$). These findings implicated heterozygous *Gata4* knockout in the SHF for AV septation, with temporal requirements mirroring those previously described for Hh signaling (32).

Interestingly, AVSDs were not observed in SHF-specific *Gata4* heterozygous mice generated with an alternate SHF-expressing Cre line, *Mef2cAHF*. Neither *Mef2cAHF::Cre* $Gata4^{fl/+}$ embryos (1/22) (Fig. 1 *M* and *R*) nor littermate control $Gata4^{fl/+}$ embryos (0/15) demonstrated AVSDs at E13.5 (Fig. 1 *I* and *N* and Table 2). Thus, AVSD penetrance was high using $Gli1^{CreERT2}$ but not using *Mef2cAHF::Cre*. We compared SHF *Cre* expression directly in these lines and observed distinct SHF *Cre* expression domains. *Cre*-dependent *lacZ* expression from the *R26R* locus in *Mef2cAHF::Cre*;*R26R* embryos was truncated at an anterior position and did not include the posterior DMP compared with *Cre* expression from $Gli1^{CreERT2}$;*R26R* embryos at E10.5 (Fig. S3). This observation suggested that the pSHF expression domain of *Gli1CreERT2* compared with *Mef2cAHF::Cre* (34) was necessary for AVSD causation by Gata4 heterozygosity.

***Gata4* Is Required for DMP Development.** We examined the requirement for *Gata4* in the SHF for DMP development using GIFM (51). We previously demonstrated that the DMP is derived from Hh signal-receiving atrial septum progenitors, marked in *R26R*;$Gli1^{Cre\text{-}ERT2/+}$ embryos by TM administration at E7.5 and E8.5 and evaluated by *β-gal* expression at E10.5 (32). *Gata4* heterozygous deletion combined with Hh-specific GIFM in $Gli1^{Cre\text{-}ERT2/+}$;$Gata4^{fl/+}$;$R26R^{fl/+}$ embryos treated with TM at E7.5 and E8.5 caused a hypoplastic or missing DMP, with qualitatively fewer marked cells (Fig. 2 *B*, *D*, *F*, and *H*) than in control $Gli1^{Cre\text{-}ERT2/+}$;$R26R^{fl/+}$ embryos (Fig. 2 *A*, *C*, *E*, and *G*) at E10.5. These results demonstrated the SHF requirement for *Gata4* in DMP development and suggested an intersection between *Gata4* and Hh signaling.

***Gata4* Regulates Cell-Cycle Progression of Cardiac Progenitors in the pSHF.** We hypothesized that the requirement for *Gata4* for DMP development reflected a requirement for SHF cell proliferation. We assessed proliferation by BrdU incorporation and found that *Gata4* was required for normal proliferation of Hh-receiving cells. $Gli1^{Cre\text{-}ERT2/+}$;$Gata4^{fl/+}$ embryos treated with TM at E7.5 and 8.5 demonstrated 39.1% fewer BrdU-positive SHF cells than control $Gata4^{fl/+}$ embryos at E9.5. (41.6 ± 3.36% vs. 68.2 ± 3.43%; $P = 0.002$) (compare Fig. 3*C* with Fig. 3 *D* and *E*). In contrast, we observed no *Gata4* dependence on SHF apoptosis. We assessed cell death by TUNEL staining and observed no differences in the pSHF between $Gli1^{Cre\text{-}ERT2/+}$;$Gata4^{fl/+}$ mutant and $Gata4^{fl/+}$ littermate

Table 2. Incidence of ASDs in *Gata4*-mutant embryos

Genotype	ASD	Total	Type	Vs. littermate control	*P* value
Conditional mutation of *Gata4*					
$Gata4^{+/-}$;$Ella^{Cre/+}$	7	18	All primum	vs. $Ella^{cre/+}$ (0/13)	0.0053
$Gata4^{fl/+}$;$Tnt^{Cre/+}$	0	12	—	vs. $Gata4^{fl/+}$ (0/13)	1
$Gata4^{fl/+}$; $Tie^{Cre/+}$	0	23	—	vs. $Gata4^{fl/+}$ (0/13)	1
$Gata4^{fl/+}$;$Gli1^{Cre\text{-}ERT2/+}$ (TM at E7.5 and E8.5)	13	21	All primum	vs. $Gata4^{fl/+}$ (0/15)	<0.0001
$Gata4^{fl/+}$;$Gli1^{Cre\text{-}ERT2/+}$ (TM at E8.5 and E9.5)	2	9	All primum	vs. $Gata4^{fl/+}$ (0/10)	0.0675 0.1053*
$Gata4^{fl/+}$; *Mef2cAHF::Cre*	1	22	All primum	vs. $Gata4^{fl/+}$ (0/15)	1
Tbx5–Gata4 compound mutant embryos					
$Tbx5^{fl/+}$;$Gata4^{fl/+}$; *Mef2cAHF::Cre*	3	9	1 primum 2 common atrium with CCAVC	vs. $Gata4^{fl/+}$;*Mef2cAHF::Cre* (0/13)	0.0125 0.0273*
				vs. $Tbx5^{fl/+}$;*Mef2cAHF::Cre* (0/13)	0.0125 0.0273*
Pten–Gata4 compound mutant embryos					
$Pten^{fl/+}$;$Gata4^{fl/+}$;$Gli1^{Cre\text{-}ERT2/+}$	1	10	All primum	vs. $Gata4^{fl/+}$;$Gli1^{Cre\text{-}ERT2/+}$ (4/6)	0.0179 0.0179*
				vs. $Pten^{fl/+}$;$Gli1^{Cre\text{-}ERT2/+}$ (0/18)	0.1719
Smo – Gata4 compound mutant embryos					
$Smo^{fl/+}$;$Gata4^{fl/+}$; *Mef2cAHF::Cre*	5	15	All common atrium	vs. $Gata4^{fl/+}$;*Mef2cAHF::Cre* (0/9)	0.0258 0.0590*
				vs. $Smo^{fl/+}$;*Mef2cAHF::Cre* (0/12)	0.0134 0.0235*
$Gata4^{fl/+}$,$SmoM2^{fl/+}$,$Gli1^{Cre\text{-}ERT2/+}$	1	10	All primum	vs. $SmoM2^{fl/+}$;$Gli1^{Cre\text{-}ERT2/+}$ (0/7) vs. $Gata4^{fl/+}$;$Gli1^{Cre\text{-}ERT2/+}$ (13/21)	0.3719 0.0106 0.0045*

ASDs were evaluated by the integrity and completion of the DMP and the AV cushion. Incidence of ASDs was evaluated in *Gata4*-mutant embryos at E13.5.
*If the χ^2 *P* value was significant within the range (0.01 < *P* value < 0.1), a second *P* value was reported using the one-tailed Fisher exact test.

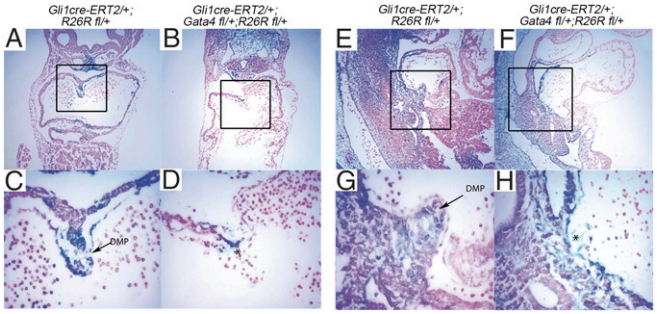

Fig. 2. *Gata4* is required for DMP development. The *Hh*-receiving cardiac fate map was abnormal in *Gata4*-mutant embryos. *Hh*-receiving cells were marked by *β-gal* expression in $Gli1^{Cre\text{-}ERT2/+}$;$R26R^{fl/+}$ embryos at E7.5 and E8.5 by TM administration and were analyzed by lacZ staining at E10.5. A marked hypoplastic or missing DMP was observed in $Gli1^{Cre\text{-}ERT2/+}$;$Gata4^{fl/+}$;$R26R^{fl/+}$ embryos (*C*, *D*, *G*, and *H*) compared with the $Gli1^{Cre\text{-}ERT2/+}$;$R26R^{fl/+}$ embryos (*A*, *B*, *E*, and *F*). *C*, *D*, *G*, and *H* show the boxed areas in *A*, *B*, *E*, and *F*, respectively, at higher magnification. (Magnification: 100× in *A*, *B*, *E*, and *F*; 400× in *C*, *D*, *G*, and *H*.)

control embryos (Fig. 3 *F*–*I*). Together, these findings define a requirement for *Gata4* in the proliferation but not in the survival of pSHF cardiac progenitors.

We analyzed the role of *Gata4* in SHF cell-cycle progression. We identified cells in specific phases of the cell cycle by IHC for the mitotic marker phosphohistone H3 (H3S10) [punctate in G2 phase (Fig. 4*E*, black arrowheads) and homogeneous in M phase (Fig. 4*E*, red arrowheads] (35, 52) and the G1-S phase marker Cdk4. We observed a 43.5% reduction of cells in G2 phase (6.99 ± 0.59% vs.12.35 ± 1.06%, $P = 0.03$) and a 32.1% reduction of cells in M phase (5.52 ± 0.52% vs. 8.13 ± 0.41%, $P = 0.04$) (Fig. 4*F*) in the pSHF of $Gli1^{Cre\text{-}ERT2/+}$;$Gata4^{fl/+}$ embryos (Fig. 4 *B* and *D*) compared with $Gata4^{fl/+}$ embryos (Fig. 4 *A* and *C*) at E10.5. We also observed a 44.5% reduction of cells in G1-S, marked by Cdk4, in the pSHF of $Gli1^{Cre\text{-}ERT2/+}$;$Gata4^{fl/+}$ embryos (Fig. 4 *H*, *J*, and *K*) compared with $Gata4^{fl/+}$ littermate controls (25.7 ± 8.21% vs. 46.3 ± 5.26%, $P = 0.028$) (Fig. 4 *G*, *I*, and *K*). We investigated the molecular basis of the requirement for *Gata4* for cell-cycle progression by examining the pSHF expression of *Cdk4*, *Cdk6*, *Cdk2*, *Cyclin D2*, *Cdkn1a*, and *Pten*, which are responsible for G1-S phase transition. We observed that the expression of *Cdk4*, *Cdk6*, and *Cyclin D2* was decreased in the pSHF of $Gli1^{Cre\text{-}ERT2/+}$;$Gata4^{fl/+}$ embryos by 34.6, 34.5, and 30.7%, respectively, compared with $Gata4^{fl/+}$ littermate controls at E9.5 by real-time PCR (0.693 ± 0.074, $P = 0.008$; 0.642 ± 0.112, $P = 0.007$; and 0.645 ± 0.125, $P = 0.022$, respectively) (Fig. 4*L*). These results establish *Gata4* as a driver of cell-cycle progression in SHF cardiac progenitors in addition to its known role in the cell-cycle progression of cardiomyocytes (1).

Genetically Targeted Disruption of *PTEN* Expression in Atrial Septum Progenitors Rescued ASDs in *Gata4*-Mutant Embryos. Pten is a tumor suppressor and is a well-established negative regulator of cell-cycle progression (53, 54) and *Cyclin D* expression (55–57). RNA-seq indicated that *Pten* was expressed extensively in heart and SHF (Table 2). We therefore hypothesized that a normal *Gata4* and *Pten* balance may be required for proper SHF cell-cycle control and, furthermore, that reduction of *Pten* activity may rescue AVSDs caused by decreased *Gata4* activity in the SHF. We tested this hypothesis by combining conditional dominant *Gata4* knockout with dominant *Pten* knockout in the SHF using *Gli1Cre:ERT2*. In control $Gli1^{Cre\text{-}ERT2/+}$;$Pten^{fl/+}$ embryos treated with TM at E7.5 and E8.5, normal atrial septation was always observed at E14.5 (18/18) (Fig. 5 *A* and *D*). In $Gli1^{Cre\text{-}ERT2/+}$;$Gata4^{fl/+}$;$Pten^{fl/+}$ embryos, conditional *Pten* haploinsufficiency rescued AVSDs observed in littermate $Gli1^{Cre\text{-}ERT2/+}$;$Gata4^{fl/+}$ embryos (1/10 vs. 4/6 AVSDs, $P = 0.0179$ (χ^2 test) or 0.0288 (one-tailed Fisher exact test) (compare Fig. 5 *C* and *F* with Fig. 5 *B* and *E* and see Table 2).

We tested whether *Pten* haploinsufficiency restored cell-cycle progression as a mechanism for rescue of AVSDs caused by

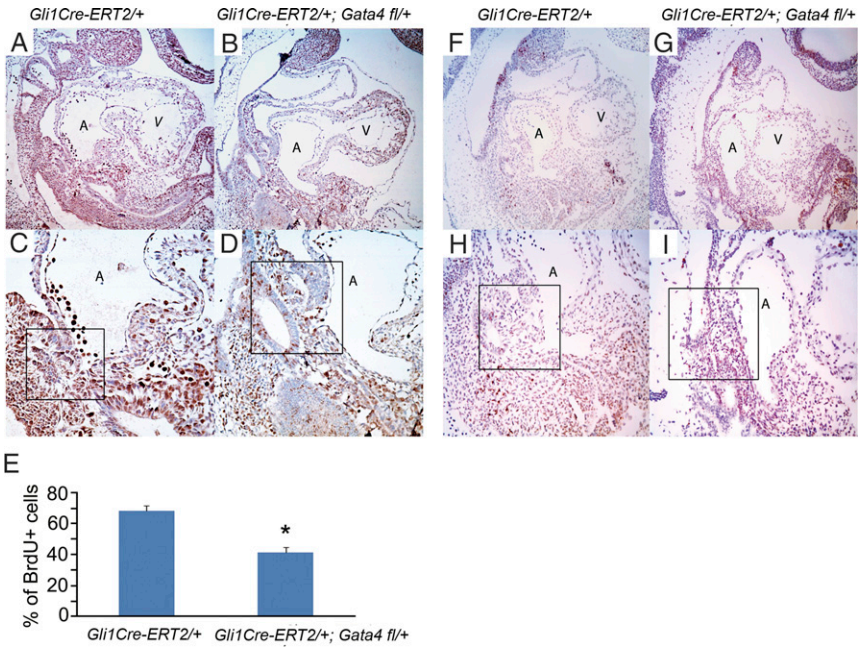

Fig. 3. *Gata4* is required for the proliferation but not for the survival of atrial septum progenitors. (*A*–*D*) BrdU staining was performed in $Gli1^{Cre\text{-}ERT2/+}$;$Gata4^{fl/+}$ embryos (*B* and *D*) and $Gli1^{Cre\text{-}ERT2/+}$ embryos (*A* and *C*) at E9.5. (*E*) The percent of cardiac progenitors that incorporated BrdU in the pSHF and the DMP region (typical regions are shown as the boxed areas in *C*, *D*, *H*, and *I*) was calculated in a total of 500 cells, counted in five serial sections. Data are presented as mean ± SEM, $n = 3$ or 4; $^*P < 0.05$. (*F*–*I*) TUNEL staining was performed in $Gli1^{Cre\text{-}ERT2/+}$;$Gata4^{fl/+}$ embryos (*G* and *I*) and $Gli1^{Cre\text{-}ERT2/+}$ littermate control embryos (*F* and *H*) at E9.5. (Magnification: 100× in *A*, *B*, *F*, and *G*; 200× in *C*, *D*, *H*, and *I*.) A, atrium; V, ventricle.

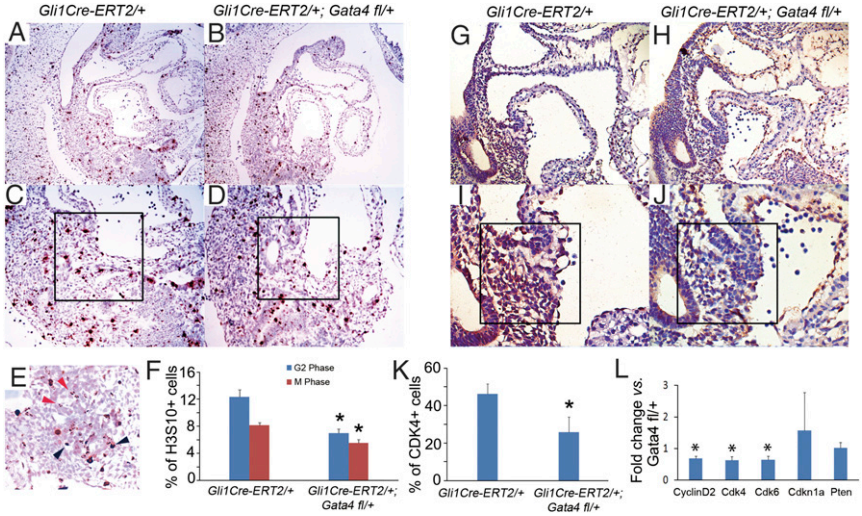

Fig. 4. *Gata4* regulates cell-cycle progression of pSHF. (*A–D*) IHC staining for H3S10 was performed in the pSHF of the $Gata4^{Gli1Cre\text{-}ERT2/+}$ embryos (*B* and *D*) and in $Gli1^{Cre\text{-}ERT2/+}$ embryos (*A* and *C*) at E9.5. (*E*) The black arrowheads indicate typical cells in M phase; the red arrowheads indicate typical cells in G2 phase. (*F*) The percentage of $H3S10^{+}$ cardiac progenitors was calculated in 500 cells in the pSHF and the DMP region (typical regions are shown as the boxed areas in *C* and *D*) counted in five serial sections. Data are presented as mean ± SEM, $n = 3$ or 4; $^{*}P < 0.05$. (*G–J*) IHC staining for Cdk4 was performed in $Gli1^{Cre\text{-}ERT2/+}$; $Gata4^{fl/+}$ embryos (*H* and *J*) and in $Gli1^{Cre\text{-}ERT2/+}$ embryos (*G* and *I*) at E9.5. (*K*) The percentage of $Cdk4^{+}$ cardiac progenitors was calculated in 500 cells in the pSHF and the DMP region (typical regions are shown as the boxed areas in *I* and *J*) counted in five serial sections. Data are presented as mean ± SEM, $n = 3$ or 4; $^{*}P < 0.05$. (*L*) Expression levels of cell-cycle–related genes in the pSHF of mouse embryos at E9.5 were measured by real-time PCR. Data are presented as mean ± SEM, $n = 3$; $^{*}P < 0.05$. (Magnification: 100× in *A*, and *B*; 200× in *C*, and *D*; 400× in *E*; 150× in *G* and *H*; 300× in *I* and *J*.)

dominant Gata4 knockout. We analyzed the percentage of G2- and M-phase cells in the pSHF in the presence or absence of *Pten* haploinsufficiency in $Gli1^{Cre\text{-}ERT2/+}$;$Gata4^{fl/+}$ embryos at E9.5 by IHC staining of H3S10 (Fig. 5 *G–L* and *S*). The G2-phase and M-phase cell-cycle defects in $Gli1^{Cre\text{-}ERT2/+}$;$Gata4^{fl/+}$ embryos were rescued in $Gli1^{Cre\text{-}ERT2/+}$;$Gata4^{fl/+}$;$Pten^{fl/+}$ embryos (for G2 phase, 5.33 ± 0.58% vs. 10.2 ± 0.76%, $P = 0.001$; for M phase, 5 ± 0.5% vs. 9.67 ± 0.58%, $P = 0.001$) (Fig. 5*S*) and cell-cycle parameters were restored to those observed in control $Gli1^{Cre\text{-}ERT2/+}$ embryos (11.2 ± 0.29% for G2 phase, $P = 0.074$; 9.33 ± 0.58% for M phase, $P = 0.422$) (Fig. 5*S*). We further observed that the defects in cell-cycle gene expression observed in *Gata4*-mutant embryos (Fig. 5 *M–R* and *T*) were rescued by decreased *Pten* dose. IHC staining for *Cdk4* expression in pSHF of $Gli1^{Cre\text{-}ERT2/+}$;$Gata4^{fl/+}$;$Pten^{fl/+}$ embryos (44.3 ± 3.85%) (Fig. 5 *O* and *R*) was normalized to levels observed in control $Gli1^{Cre\text{-}ERT2/+}$ embryos (46.3 ± 4.80%, $P = 0.66$) (Fig. 5 *M* and *P*). We next analyzed the pSHF RNA expression of cell-cycle regulators in $Gli1^{Cre\text{-}ERT2/+}$;$Gata4^{fl/+}$, $Gli1^{Cre\text{-}ERT2/+}$;$Pten^{fl/+}$, or $Gli1^{Cre\text{-}ERT2/+}$;$Gata4^{fl/+}$;$Pten^{fl/+}$ embryos at E9.5. As expected, we observed decreased expression of *Gata4*, *Cdk6*, *Cdk4*, and *Ccnd2* in the pSHF of $Gli1^{Cre\text{-}ERT2/+}$;$Gata4^{fl/+}$ embryos and decreased expression of *Pten* but significantly higher expression of *Cdk6* and *Cdk4* in the pSHF of $Gli1^{Cre\text{-}ERT2/+}$;$Pten^{fl/+}$ embryos (Fig. 5*U*). Compound heterozygous knockout of *Gata4* and *Pten* restored the SHF expression of *Cdk6* and *Cdk4* to normal levels observed in control $Gata4^{fl/+}$ embryos, rescuing the expression decrement caused by heterozygous loss of *Gata4* alone (Fig. 5*U*). Together these findings implicate a *Gata4*/*Pten* balance in cell-cycle control in the SHF for AV septation.

***Gata4* Interacts with *Tbx5* in AV Septation.** Because *Gata4* interacts genetically with *Tbx5* for normal cardiac morphogenesis (3), and each is independently required in the SHF for AV septation (Fig. 1) (35), we hypothesized that these transcription factor genes may interact genetically in the SHF. We created SHF-specific *Gata4* and *Tbx5* haploinsufficiency using the SHF-specific *Mef2cAHF::Cre* BAC transgenic mouse line ($Tbx5^{fl/+}$;$Gata4^{fl/+}$;*Mef2cAHF::Cre*). $Tbx5^{fl/+}$;$Gata4^{fl/+}$;*Mef2cAHF::Cre* embryos had a higher incidence of AVSDs than seen in littermate single $Gata4^{fl/+}$;*Mef2cAHF::Cre* or $Tbx5^{fl/+}$;*Mef2cAHF::Cre* embryos at E13.5 (3/9, 0/13, and 0/13, respectively) (Table 2) ($Tbx5^{fl/+}$;$Gata4^{fl/+}$;*Mef2cAHF::Cre* vs. $Gata4^{fl/+}$;*Mef2cAHF::Cre*, $P = 0.0125$ by χ^2 test or 0.0273 by one-tailed Fisher exact test; $Tbx5^{fl/+}$;$Gata4^{fl/+}$;*Mef2cAHF::Cre* vs. $Tbx5^{fl/+}$;*Mef2cAHF::Cre*, $P = 0.0125$ by χ^2 test or 0.0273 by one-tailed Fisher exact test). Furthermore, we observed more severe AVSDs [including a common atrium and complete common AV canal (CCAVC) (Fig. 6 *A–C* and *A′–C′* and Table 2)] in compound $Tbx5^{fl/+}$;$Gata4^{fl/+}$;*Mef2cAHF::Cre* embryos than in single heterozygotes. Therefore, *Gata4* and *Tbx5* interact genetically in the SHF or in SHF-derived cells for AV septation.

***Gata4* Interacts with *Hh* signaling in AV Septation.** The requirement of *Gata4* in *Hh*-receiving cells for AV septation (Fig. 1) suggested that *Gata4* and *Hh* signaling may interact genetically in the SHF for atrial septation. We tested this hypothesis by creating SHF compound heterozygous knockouts of *Gata4* and *Smo* using Mef2c-Cre, encoding the obligate Hh receptor ($Smo^{fl/+}$;$Gata4^{fl/+}$;*Mef2cAHF::Cre*). No ASDs or AVSDs were observed in $Smo^{fl/+}$;*Mef2cAHF::Cre* embryos (0/12) (Fig. 6 *D* and *D′*) or in $Gata4^{fl/+}$;*Mef2cAHF::Cre* embryos (0/9) (Fig. 6 *B* and *B′*) at E13.5. In contrast, severe AVSDs, including common atrium and CCAVC, were observed in 33% (5/15) of $Smo^{fl/+}$;$Gata4^{fl/+}$;*Mef2cAHF::Cre* embryos at E13.5 [$P = 0.0258$ (χ^2 test) or 0.0590 (Fishers exact test) vs. $Gata4^{fl/+}$;*Mef2cAHF::Cre* and $P = 0.0125$ (χ^2 test) or 0.0273 (Fishers exact test) vs. $Smo^{fl/+}$;*Mef2cAHF::Cre*)] (Fig. 6 *E* and *E′* and Table 2). These results suggested a genetic interaction between *Gata4* and the *Hh* signaling pathway for AV septation.

We tested the hypothesis that *Gata4* was required for SHF Hh signaling by evaluating the expression of the known Hh signaling targets *Gli1* and *Osr1* and the Hh signaling components *Shh*, *Smo*, *Gli3*, and *Gas1*. *Gata4* expression in the pSHF of $Gli1^{Cre\text{-}ERT2/+}$;$Gata4^{fl/fl}$ embryos was significantly decreased as compared with $Gata4^{fl/+}$ embryos (0.446 ± 0.098, $P = 0.013$), as expected. Expression of *Gli1*, *Osr1*, and *Smo* was significantly reduced in the pSHF of $Gli1^{Cre\text{-}ERT2/+}$;$Gata4^{fl/fl}$ embryos compared with control $Gata4^{fl/+}$ embryos as determined by real-time PCR at E9.5 (0.338 ± 0.105, $P = 0.0004$; 0.440 ± 0.059, $P = 0.0008$; and 0.654 ± 0.076,

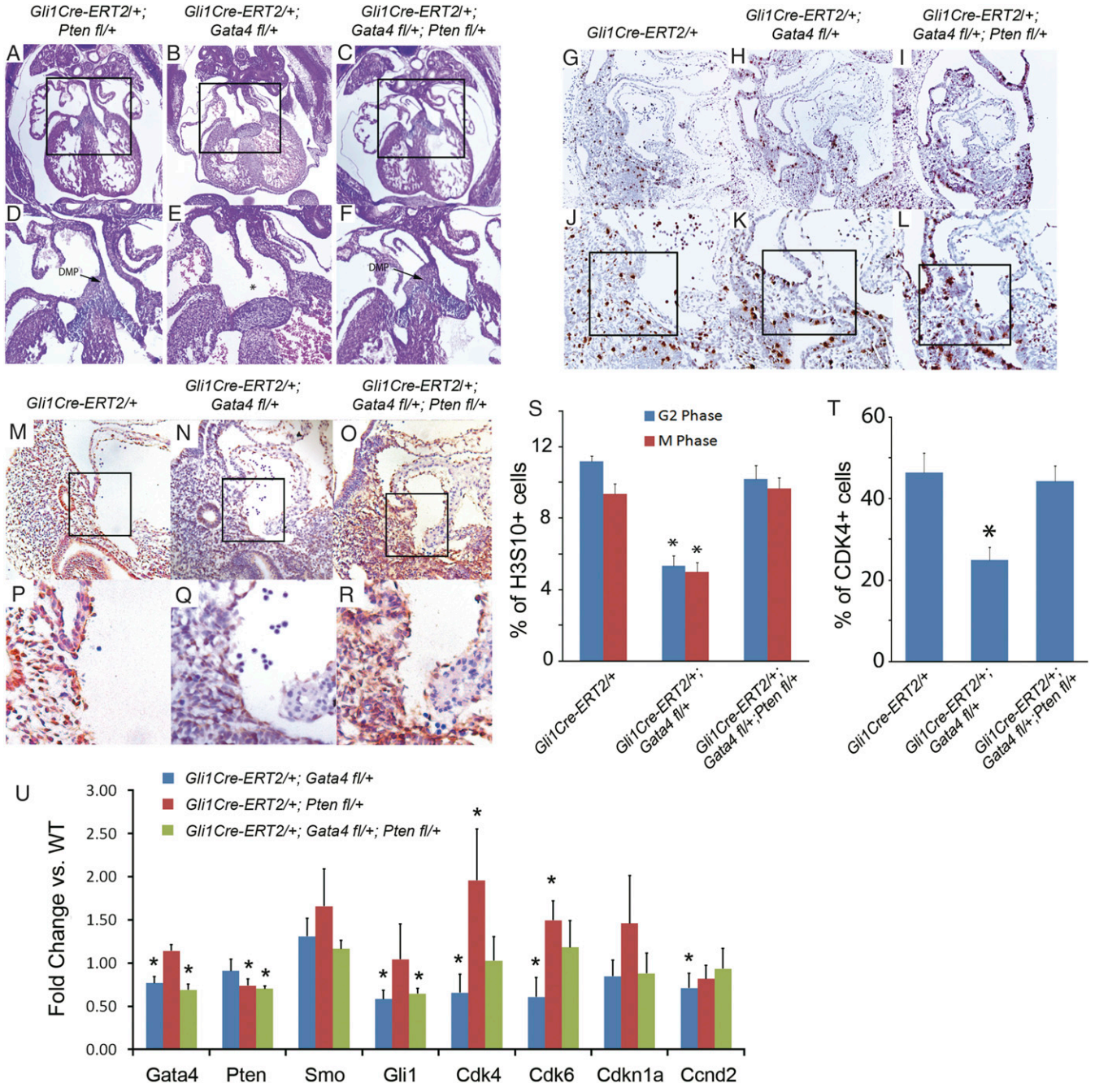

Fig. 5. Genetically targeted disruption of *Pten* expression in atrial septum progenitors rescued ASDs in *Gata4*-mutant embryos. (*A–F*) Histology of *Gata4* transgenic mouse embryo hearts at E13.5. Asterisks indicate missing structures of atrial septation. *D–F* show the boxed areas in *A–C* at greater magnification. (Magnification: 40× in *A–C*; 100× in *D-F*.) (*G–L*) IHC staining for H3S10 was performed on $Gli1^{Cre\text{-}ERT2/+}$;$Gata4^{fl/+}$;$Pten^{fl/+}$ (*I* and *L*), $Gli1^{Cre\text{-}ERT2/+}$;$Gata4^{fl/+}$ (*H* and *K*), and $Gli1^{Cre\text{-}ERT2/+}$ (*G* and *J*) embryos at E9.5. (Magnification: 100× in *G–I*; 200× in *J–L*.) (*M–R*) IHC staining for H3S10 was performed on $Gli1^{Cre\text{-}ERT2/+}$;$Gata4^{fl/+}$;$Pten^{fl/+}$ (*O* and *R*), $Gli1^{Cre\text{-}ERT2/+}$;$Gata4^{fl/+}$ (*N* and *Q*), and $Gli1^{Cre\text{-}ERT2/+}$ (*M* and *P*) embryos at E9.5. *P–R* show the boxed areas in *M–O*, respectively, at higher magnification. (Magnification: 200× in *M–O*; 400× in *P–R*.) (*S* and *T*) The percentage of $H3S10^+$ (*S*) or $Cdk4^+$ (*T*) cardiac progenitors was calculated in 500 cells in the pSHF and the DMP region (typical regions are shown as the boxed areas in *J–L*) counted in five serial sections. Data are presented as mean ± SEM, $n = 3$; $^*P < 0.05$. (*U*) Gene expression in the pSHF of $Gli1^{Cre\text{-}ERT2/+}$;$Gata4^{fl/+}$, $Gli1^{Cre\text{-}ERT2/+}$;$Pten^{fl/+}$, or $Gli1^{Cre\text{-}ERT2/+}$;$Gata4^{fl/+}$;$Pten^{fl/+}$ embryos was measured by real-time PCR and was compared with the expression in wild-type embryos. $^*P < 0.05$.

$P = 0.0067$, respectively) (Fig. 6*F*). Other Hh pathway genes that are not known direct Hh targets, such as *Shh* and *Gli3*, were unchanged. These results suggested that Gata4 heterozygous knockout caused quantitative Hh signaling defects.

We asked if *Pten* expression was dependent on Hh signaling in pSHF. *Pten* expression was unaltered in the pSHF of *Smo* heterozygote or *Smo*-knockout mouse embryos at E9.5 compared with that in wild-type control littermates (Fig. 6*G*). Reciprocally, we asked if Hh pathway gene expression was dependent on *Pten* activity. We observed that the expression of neither *Gli1* nor *Smo* was altered by *Pten* heterozygous knockout (Fig. 5*U*). The data suggested that *Pten* expression was independent of Hh signaling and that Hh signaling pathway gene expression is independent of *Pten* activity.

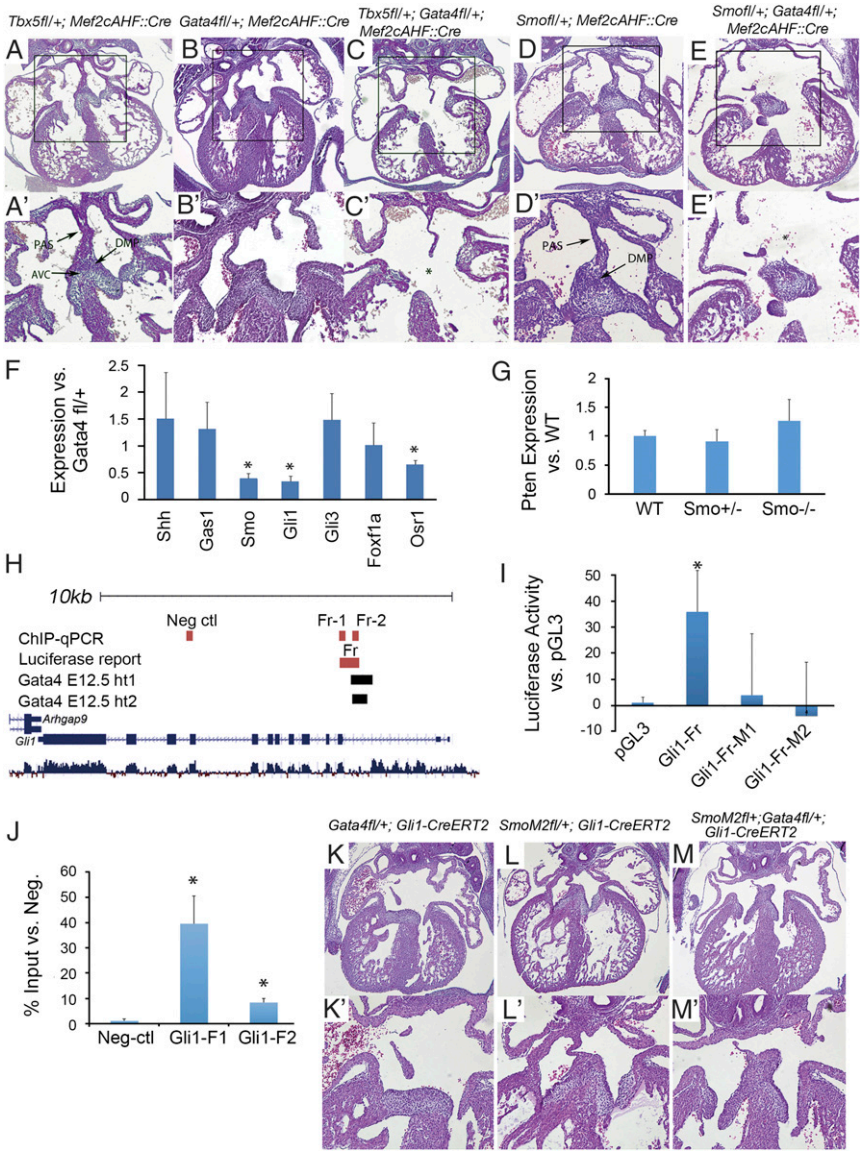

Fig. 6. *Gata4* interacts with Hh signaling in AV septation. (*A*–*E*) Histology of *Gata4* transgenic mouse embryo hearts at E14.5. Asterisks indicate missing structures of atrial septation. *A*′–*E*′ show the boxed areas in *A*–*E* at higher magnification. (Magnification: 40× in *A*–*E*; 100× in A′–E′.) (*F*) Gene expression in the pSHF of $Gli1^{Cre\text{-}ERT2/+}$;$Gata4^{fl/fl}$ embryos was measured by real-time PCR and was compared with gene expression in $Gata4^{fl/+}$ embryos. (*G*) Gene expression in the pSHF of $Smo^{+/-}$ or $Smo^{-/-}$ embryos was measured by real-time PCR and was compared with the gene expression in wild-type embryos. (*H*) Schematic of the mouse Gli1 genomic locus including Gata4-binding regions and the cloned genomic fragments used for Gata4 regulation assays (luciferase reporter assay and ChIP-qPCR). (*I*) Gata4-stimulated firefly luciferase expression is seen in wild-type Gli1-Fr but not in mutated Gli1-Fr-M1 and Gli1-Fr-M2 fragments. Results are presented as mean ± SEM; $n = 3$; $^*P < 0.05$ compared with pGL3. (*J*) Enrichment of Gata4-responsive Gli1 genomic fragments in the SHF by Gata4 ChIP-qPCR. Results are presented as mean ± SEM; $n = 3$; * $P < 0.05$. (*K*–*M*) Histology of *Gata4* transgenic mouse embryo hearts at E14.5. Asterisks indicate missing structures of atrial septation. (Magnification 40× in *K*–*M*; 100× in *K*′–*M*′.)

We hypothesized that Gata4 may regulate Hh signaling components directly. We bioinformatically interrogated the *Smo*, *Osr1*, and *Gli1* loci for potential Gata4-responsive elements. We used the overlap of evolutionary conservation and Gata4 occupancy in HL-1 cells or embryonic mouse hearts (58, 59) and identified conserved Gata4-binding sites within the second intron of *Gli1* (Fig. 6*H* and Table 3). We tested the conserved region including the Gata4-binding sites for *cis*-regulatory activity by luciferase reporter assay. Gata4 expression significantly transactivated firefly luciferase expression from this genomic construct in HEK293 cells (Fig. 6*I*). Mutant constructs, each ablating one Gata4-binding site, failed to activate luciferase expression (Fig. 6*I*). We next assessed whether Gata4 physically occupied the *Gata4*-responsive region at *Gli1* in the SHF in vivo during atrial septum progenitor specification at E9.5. ChIP-quantitative PCR (qPCR) was performed for Gata4 using microdissected SHF tissues of wild-type mouse embryos at E9.5. We observed significant enrichment of the Gata4-dependent enhancer at Gli1 but not of control fragments from neighboring upstream or downstream genomic regions (Fig. 6*J* and Table 3). Together, these results place Gata4 upstream of *Gli1*, an effector of Hh signaling activation, in the SHF.

To elucidate the in vivo hierarchy between Gata4 and Hh signaling, we combined conditional dominant Gata4 knockout in Hh-receiving cells with *Gli1:Cre*-dependent expression of SmoM2, a constitutively activated Smo mutant (60). In control $Gli1^{Cre\text{-}ERT2/+}$; $R26\text{-}SmoM2^{fl/+}$ embryos, normal septation was observed at E14.5 (7/7) (Fig. 6 *L* and *L*′). In contrast to the $Gli1^{Cre\text{-}ERT2/+}$;$Gata4^{fl/+}$ embryos (13/21) that showed AVSDs, only 1/10 of $Gata4^{fl/+}$;

Table 3. Genomic regions with Gata4-binding sites assessed by luciferase reporter assay and ChIP-qPCR

	Luciferase assay				ChIP		
Gene name	Genomic fragment	Locus	Luciferase results	Gata4-binding sites in subcloned fragments	Genomic fragment	Locus	ChIP results, % of input
Gli1	Gli1-Fr	chr10:126775570–126776129	42.1 ± 16.2, $P = 0.0478$	chr10:126775655–126775660 chr10:126776103–126776108	Gli1-Fr1	chr10:126775576–126775736	0.44 ± 0.12, $P = 0.0039$
	Gli-Fr-M1		6.3 ± 25.8, $P = 0.4711$	chr10:126776103–126776108*	Gli1-Fr2	chr10:126775984–126776129	0.09 ± 0.01, $P = 0.0163$
	Gli1-Fr-M2		−6.3 ± 22.3, $P = 0.4270$	chr10:126775655–126775660*	Negative control	chr10:126771190–126771322	0.01 ± 0.01

All genomic coordinates are shown in mouse genome build mm9.
*This site was deleted in the mutated subclone of the Gata4 fragment.

Gli1$^{Cre\text{-}ERT2/+}$;*R26-SmoM2*$^{fl/+}$ embryos showed ASVDs, indicating significant rescue by *R26-SmoM2* (P = 0.0106 by χ^2 test or $P = 0.0045$ by one-tailed Fisher exact test) (compare Fig. 6 *M* and *M′* with Fig. 6 *K* and *K′* and see Table 2). Rescue of AVSDs in *Gata4*-mutant embryos by constitutive Hh signaling was consistent with the molecular data placing *Gata4* upstream of Hh signaling in SHF atrial septum progenitors.

Discussion

Dominant mutations in the essential cardiogenic transcription factors including Gata4, Tbx5, and Nkx2-5 cause human atrial and AVSDs; however, the gene-regulatory networks required for atrial septation downstream of these essential transcription factors have remained unidentified. Here we have implicated *Gata4* in the SHF for atrial/AV septation and have defined genetic interactions between Gata4 and both Hh signaling and Pten for cardiac septation. Our study provides genetic, cellular, and molecular evidence supporting a dosage-sensitive requirement for *Gata4* in SHF progenitors. Support for a SHF role of *Gata4* in atrial septation includes the observation that *Gata4* is required in Hh signal-receiving SHF progenitor cells. Use of the TM-inducible *Gli1*^{CreERT2} allowed the temporal requirement for *Gata4* to be ascertained: *Gli1-CreERT2* activation by TM treatment at E7.5 and E8.5 caused penetrant AVSDs, but TM treatment at E8.5 and E9.5 did not. This result suggests that Gata4 is required in SHF Hh-receiving progenitors for AV septation but not at a later time in SHF-derived myocardium. This temporal requirement mirrors that previously observed for Hh signaling in the SHF (32). Together, these observations suggest an essential role for *Gata4* in SHF Hh-receiving cardiac progenitors for atrial septation. This work joins our previous work implicating *Tbx5* and Hh signaling and the work of others implicating Wnt and Bmp signaling in the SHF for AV septation, providing support for the importance of SHF pathways in AVSD causation (32, 34–36, 61, 62). These studies imply that disrupted SHF gene regulatory networks play an important role in the ontogeny of AVSDs and should be considered by groups working to identify the genetic causation of AVSDs in humans.

Our observations do not preclude a requirement for *Gata4* in myocardium or endocardium in atrial septation, despite the absence of defects in embryos with conditional dominant *Gata4* knockout generated by myocardial-specific *Tnt:Cre* or endocardial-specific *Tie2:Cre*. In fact, previous studies have identified interactions between *Gata4* and other genes essential for cardiac septation in other lineages. For example, lineage-specific *Gata4* and *Tbx5* heterozygosity in endocardium (63) or myocardium (4) caused ASDs and AVSDs, respectively, demonstrating a combinatorial requirement for *Gata4* and *Tbx5* in these lineages. *Gata4* is highly expressed in the SHF in a pattern overlapping with *Tbx5* (13, 39), and we observed that *Gata4* and *Tbx5* interact genetically in the SHF for atrial septation (Fig. 6). GATA4 and TBX5 interact physically to activate gene expression synergistically in the heart (2), and multiple *Gata4* transcriptional targets have been identified in the heart (1, 4, 5, 7, 22, 64). Recent studies have indicated that GATA4 and TBX5 are essential for each other's transcriptional fidelity in the control of cardiac gene regulatory networks in mouse and human models (65, 66). Determining GATA4 and TBX5 coregulated targets in the SHF may identify genes essential for normal atrial septum morphogenesis.

Gata4 directly regulates the transcription of cell-cycle genes in the myocardium (1, 67). We observed that *Cyclin D2*, *Cdk4*, and *Cdk6* are *Gata4* dependent in the SHF. Diminished expression of cell-cycle control genes in the SHF was a plausible molecular mechanism for AVSD causation in *Gata4* mutants. In support of this hypothesis, SHF-specific knockdown of *Pten*, a tumor suppressor that negatively regulates *Cdk4* and *Cdk6*, rescued atrial septation in *Gata4* mutants. These observations support a model in which *Gata4* drives SHF progenitor proliferation to generate a progenitor pool capable of supporting atrial septum morphogenesis. The *Pten* rescue experiments describe a balance between SHF *Gata4* and *Pten* dose required for proper expansion of atrial septum progenitors, integrating cardiogenic transcription factor and cell-cycle regulatory genes in an SHF pathway for AV septation (Fig. 7).

We provide evidence that *Gata4* acts upstream of Hh signaling in atrial septation (Fig. 7). *Gata4* and *Smo* interact genetically, and, remarkably, SHF-specific constitutive Hh signaling rescued AVSDs in *Gata4*-mutant embryos (Fig. 6). Genetic rescue suggested a *Gata4–Hh* signaling hierarchy, which we identified molecularly: *Gata4* mutants have diminished SHF Hh signaling, because Hh signaling components, including the known Hh target genes *Gli1* and *Osr1*, demonstrated *Gata4*-dependent pSHF expression. Furthermore,

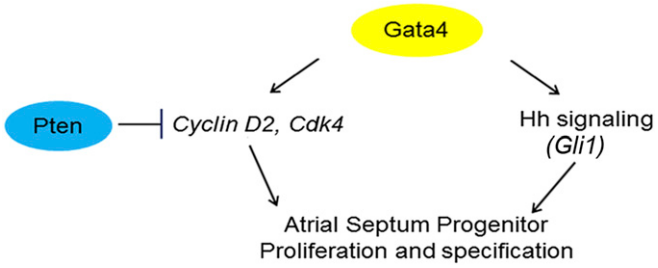

Fig. 7. Model of *Gata4* transcriptional regulation in atrial septation. *Gata4* acts upstream of both *Hh* signaling and the *Pten*/*Cdk4*/*Cyclin D2* pathways. These pathways appear to be independent, and rescue of either pathway prevents CHDs in *Gata4* heterozygote knockouts, supporting a model in which combined deficiency of both pathways is required for CHD pathogenesis.

we identified Gata4-responsive *cis*-regulatory elements at *Gli1* that were occupied by GATA4 in vivo, providing evidence that *Gli1* is a direct GATA4 SHF target. Together these observations support a model in which *Gata4* is required upstream of SHF Hh signaling for atrial septation (Fig. 7).

The mechanism whereby dominant transcription factor mutations cause developmental phenotypes remains largely unanswered. We have linked *Gata4* to two distinct molecular pathways in vivo, *Pten*-modulated cell cycle and Hh signaling. Our prior work suggested that Hh signaling was required for SHF patterning but not for proliferation for AV septation (33), and transcriptional profiling for SHF Hh-dependent gene expression did not uncover genes required for proliferation (44). Furthermore, *Pten* expression in not altered in Hh pathway mutants, and, reciprocally, Hh pathway gene expression is not altered in *Pten* mutants, suggesting that these pathways function independently. Interestingly, ASDs caused by *Gata4* heterozygous knockout were rescued by restoring cell-cycle transition (using *Pten* knockdown; Fig. 5) or by constitutive Hh signaling (Fig. 6). Because restoration of either pathway restored normal cardiac morphogenesis and prevented CHD, we concluded that both the cell-cycle and Hh signaling decrements were required for *Gata4*-dependent CHD. Together these observations suggest that deficiency of multiple, discrete target pathways downstream of *Gata4* are required in combination for CHD pathogenesis caused by dominant *Gata4* transcription factor mutations, suggesting a combinatorial model for disease causation by transcription factor haploinsufficiency.

Materials and Methods

Mouse Lines. All mouse experiments were performed in a mixed B6/129/SvEv background. The $Gata4^{fl/fl}$ mouse line was a kind gift from the laboratory of William Pu, Harvard University, Cambridge, MA. $Tbx5^{fl/+}$, $Gli1^{CreERT2/+}$, *Mef2cAHF::Cre*, $Tie2^{Cre/+}$, and $Smo^{fl/+}$ mouse lines were obtained from the I.P.M. laboratory. The $TnT^{Cre/+}$ mouse line was from the laboratory of Yiping Chen, Tulane University, New Orleans. Generation and genotyping of the $Gata4^{fl/fl}$, $Tbx5^{fl/+}$, $Gli1^{CreERT2/+}$, $Tie2^{Cre/+}$, $TnT^{Cre/+}$, and *Mef2cAHF::Cre* mouse lines have been reported (8, 35, 49, 50, 68–70). $Pten^{fl/+}$ and $Ella^{cre/+}$ mouse lines were purchased from the Jackson Laboratory. Mouse experiments were performed according to a protocol reviewed and approved by the Institutional Animal Care and Use Committee of the University of North Dakota, in compliance with the US Public Health Service Policy on the Humane Care and Use of Laboratory Animals.

TM Administration and X-Gal Staining. TM-induced activation of *CreERT2* was accomplished by oral gavage with two doses of TM (75 mg/kg) at E7.5 and E8.5 (32). X-gal staining of embryos was performed as described (32).

IHC. Standard procedures were used for histology and IHC. IHC was performed using the antibodies rabbit anti-mouse p-Histone-H3 (H3S10) (Abcam) and rabbit anti-mouse CDK4 (Abcam). For colorimetric staining, slides were incubated with rabbit ImmPress reagent (Vector Labs), developed using a 3,3′-diaminobenzidine-tetrahydrochloride (DAB) substrate kit (Vector Labs), and counterstained with hematoxylin. For BrdU incorporation, pregnant mice were given 100 mg BrdU/kg body weight in 10 mg/mL solutions at E9.0 in two doses, 3 h and 6 h, respectively, before the animals were killed. BrdU staining was performed using a BrdU In-Situ Detection Kit (EMD Millipore). For TUNEL staining, an ApopTag Plus Peroxidase in-Situ Apoptosis Detection Kit was used (EMD Millipore).

Microdissection of pSHF and RNA Extraction. To obtain the pSHF splanchnic mesoderm for use in real-time qPCR, E9.5 embryos were dissected as described previously (35, 44). The heart, aSHF, and pSHF were collected separately in RNAlater RNA Stabilization Reagent (QIAGEN) and then were stored at −20 °C until genotyping was completed.

Real-Time PCR. Total RNA was extracted from the pSHF regions of mouse embryo hearts using the RNeasy Mini Kit (QIAGEN) according to the manufacturer's instructions. Two hundred nanograms of total RNA was reverse transcribed using a SuperScript III Reverse Transcriptase kit from Invitrogen. The qPCR was performed using a Power SYBR Green PCR Master Mix from Applied Biosystems. Results were analyzed using the ΔΔCt method with *GAPDH* as a normalization control.

Luciferase Reporter Assay. Amplified promoter regions as noted in *Results* were cloned into pGL3 Basic vector (Promega) modified to include a minimal TA promoter. Gata4 was cloned into a pcDNA3 vector. Transient transfections were performed in HEK293T cells using FuGENE HD (Promega) according to the manufacturer's instructions. Total cell lysates were prepared 48 h post-transfection, and luciferase activity was assessed using the Promega Dual Luciferase Reporter kit (Promega) according to the manufacturer's protocol.

Site-Directed Mutagenesis. Mutant reporter vectors were generated by deleting Gata4-binding sites using the QuikChange Lightning Site-Directed Mutagenesis Kit (Agilent Technologies). The following primers were used: Gli1-del1 forward (5′-GGAACGAAACAGAGAATGACAGTTTCAGGC-3′), reverse (5′-GCCTGAAACTGTCATTCTCTGTTTCGTTCC-3′) and Gli1-del2 forward (5′-CCTCGTTTCAGTCCACTGGTAGGGCCAG-3′), reverse (5′-CTGGCCCTACCAGTGGACTGAAACGAGG-3′). Detailed site information is listed in Table 3.

ChIP. E9.5 embryos were microdissected in cold PBS containing Protease Inhibitor Mixture (Roche) to isolate the primitive heart region. Approximately 20 tissues were pooled as one sample. Tissues were cross-linked with 1% formaldehyde for 15 min at room temperature and terminated with glycine. After PBS washes, tissues were dissociated by shaking at 37 °C for 1–2 h at 100 rpm in collagenase type II (Gibco) solution. Sonication was performed using a Covaris S220 sonicator to generate fragments with an average size of 600 bp. Samples were incubated with Gata4 antibody (sc-1237 X; Santa Cruz) overnight at 4 °C and then were incubated with Dynabeads Protein G (Life Technologies) for 2 h, washed, and reverse cross-linked.

ACKNOWLEDGMENTS. This project was supported by NIH Grants NIH-1R15HL117238 (to L.X.) and R01 HL092153 and R01 HL124836 (to I.P.M.), by Grants 5P20RR016471-12 and 8 P20 GM103442-12 from the National Center for Research Resources (to L.X. and K.Z.), by American Heart Association Grants 13SDG14650009 (to L.X.) and 15GRNT25700195 (to K.Z.), and by Established Investigator Award 13EIA14690081 (to I.P.M.).

1. Rojas A, et al. (2008) GATA4 is a direct transcriptional activator of cyclin D2 and Cdk4 and is required for cardiomyocyte proliferation in anterior heart field-derived myocardium. *Mol Cell Biol* 28(17):5420–5431.
2. Garg V, et al. (2003) GATA4 mutations cause human congenital heart defects and reveal an interaction with TBX5. *Nature* 424(6947):443–447.
3. Maitra M, et al. (2009) Interaction of Gata4 and Gata6 with Tbx5 is critical for normal cardiac development. *Dev Biol* 326(2):368–377.
4. Misra C, Chang SW, Basu M, Huang N, Garg V (2014) Disruption of myocardial Gata4 and Tbx5 results in defects in cardiomyocyte proliferation and atrioventricular septation. *Hum Mol Genet* 23(19):5025–5035.
5. Misra C, et al. (2012) Congenital heart disease-causing Gata4 mutation displays functional deficits in vivo. *PLoS Genet* 8(5):e1002690.
6. Rajagopal SK, et al. (2007) Spectrum of heart disease associated with murine and human GATA4 mutation. *J Mol Cell Cardiol* 43(6):677–685.
7. Dodou E, Verzi MP, Anderson JP, Xu SM, Black BL (2004) Mef2c is a direct transcriptional target of ISL1 and GATA factors in the anterior heart field during mouse embryonic development. *Development* 131(16):3931–3942.
8. Pu WT, Ishiwata T, Juraszek AL, Ma Q, Izumo S (2004) GATA4 is a dosage-sensitive regulator of cardiac morphogenesis. *Dev Biol* 275(1):235–244.
9. Zeisberg EM, et al. (2005) Morphogenesis of the right ventricle requires myocardial expression of Gata4. *J Clin Invest* 115(6):1522–1531.
10. Bisping E, et al. (2006) Gata4 is required for maintenance of postnatal cardiac function and protection from pressure overload-induced heart failure. *Proc Natl Acad Sci USA* 103(39):14471–14476.
11. Rivera-Feliciano J, et al. (2006) Development of heart valves requires Gata4 expression in endothelial-derived cells. *Development* 133(18):3607–3618.
12. Kobayashi S, et al. (2006) Transcription factor gata4 regulates cardiac BCL2 gene expression in vitro and in vivo. *FASEB J* 20(6):800–802.
13. Kuo CT, et al. (1997) GATA4 transcription factor is required for ventral morphogenesis and heart tube formation. *Genes Dev* 11(8):1048–1060.
14. Ip HS, Wilson DB, Heikinheimo M, Leiden JM, Parmacek MS (1995) The GATA-4 transcription factor transactivates the cardiac-specific troponin C promoter-enhancer in non-muscle cells. *Adv Exp Med Biol* 382:117–124.
15. Ip HS, et al. (1994) The GATA-4 transcription factor transactivates the cardiac muscle-specific troponin C promoter-enhancer in nonmuscle cells. *Mol Cell Biol* 14(11):7517–7526.
16. Basson CT, et al. (1997) Mutations in human TBX5 [corrected] cause limb and cardiac malformation in Holt-Oram syndrome. *Nat Genet* 15(1):30–35.
17. Li QY, et al. (1997) Holt-Oram syndrome is caused by mutations in TBX5, a member of the Brachyury (T) gene family. *Nat Genet* 15(1):21–29.
18. Schott JJ, et al. (1998) Congenital heart disease caused by mutations in the transcription factor NKX2-5. *Science* 281(5373):108–111.

19. Sarkozy A, et al. (2005) Spectrum of atrial septal defects associated with mutations of NKX2.5 and GATA4 transcription factors. *J Med Genet* 42(2):e16.
20. Hirayama-Yamada K, et al. (2005) Phenotypes with GATA4 or NKX2.5 mutations in familial atrial septal defect. *Am J Med Genet A* 135(1):47–52.
21. Okubo A, et al. (2004) A novel GATA4 mutation completely segregated with atrial septal defect in a large Japanese family. *J Med Genet* 41(7):e97.
22. Morin S, Charron F, Robitaille L, Nemer M (2000) GATA-dependent recruitment of MEF2 proteins to target promoters. *EMBO J* 19(9):2046–2055.
23. Malumbres M, Barbacid M (2005) Mammalian cyclin-dependent kinases. *Trends Biochem Sci* 30(11):630–641.
24. Snarr BS, Kern CB, Wessels A (2008) Origin and fate of cardiac mesenchyme. *Dev Dyn* 237(10):2804–2819.
25. Webb S, Brown NA, Anderson RH (1998) Formation of the atrioventricular septal structures in the normal mouse. *Circ Res* 82(6):645–656.
26. Zhang XM, Ramalho-Santos M, McMahon AP (2001) Smoothened mutants reveal redundant roles for Shh and Ihh signaling including regulation of L/R asymmetry by the mouse node. *Cell* 105(6):781–792.
27. Lan Y, Liu H, Ovitt CE, Jiang R (2011) Generation of Osr1 conditional mutant mice. *Genesis* 49(5):419–422.
28. Wessels A, et al. (2000) Atrial development in the human heart: An immunohistochemical study with emphasis on the role of mesenchymal tissues. *Anat Rec* 259(3): 288–300.
29. Snarr BS, Wirrig EE, Phelps AL, Trusk TC, Wessels A (2007) A spatiotemporal evaluation of the contribution of the dorsal mesenchymal protrusion to cardiac development. *Dev Dyn* 236(5):1287–1294.
30. Snarr BS, et al. (2007) Isl1 expression at the venous pole identifies a novel role for the second heart field in cardiac development. *Circ Res* 101(10):971–974.
31. Mommersteeg MT, et al. (2006) Two distinct pools of mesenchyme contribute to the development of the atrial septum. *Circ Res* 99(4):351–353.
32. Hoffmann AD, Peterson MA, Friedland-Little JM, Anderson SA, Moskowitz IP (2009) sonic hedgehog is required in pulmonary endoderm for atrial septation. *Development* 136(10):1761–1770.
33. Lin L, Bu L, Cai CL, Zhang X, Evans S (2006) Isl1 is upstream of sonic hedgehog in a pathway required for cardiac morphogenesis. *Dev Biol* 295(2):756–763.
34. Goddeeris MM, et al. (2008) Intracardiac septation requires hedgehog-dependent cellular contributions from outside the heart. *Development* 135(10):1887–1895.
35. Xie L, et al. (2012) Tbx5-hedgehog molecular networks are essential in the second heart field for atrial septation. *Dev Cell* 23(2):280–291.
36. Briggs LE, et al. (2013) Expression of the BMP receptor Alk3 in the second heart field is essential for development of the dorsal mesenchymal protrusion and atrioventricular septation. *Circ Res* 112(11):1420–1432.
37. Zhou L, et al. (2015) Tbx5 and Osr1 interact to regulate posterior second heart field cell cycle progression for cardiac septation. *J Mol Cell Cardiol* 85:1–12.
38. Zhang KK, et al. (2016) Gene network and familial analyses uncover a gene network involving Tbx5/Osr1/Pcsk6 interaction in the second heart field for atrial septation. *Hum Mol Genet* 25(6):1140–1151.
39. Yang YP, et al. (2013) Second heart field and the development of the outflow tract in human embryonic heart. *Dev Growth Differ* 55(3):359–367.
40. Moskowitz IP, et al. (2011) Transcription factor genes Smad4 and Gata4 cooperatively regulate cardiac valve development. [corrected]. *Proc Natl Acad Sci USA* 108(10): 4006–4011.
41. Watt AJ, Battle MA, Li J, Duncan SA (2004) GATA4 is essential for formation of the proepicardium and regulates cardiogenesis. *Proc Natl Acad Sci USA* 101(34): 12573–12578.
42. Rojas A, et al. (2005) Gata4 expression in lateral mesoderm is downstream of BMP4 and is activated directly by Forkhead and GATA transcription factors through a distal enhancer element. *Development* 132(15):3405–3417.
43. Molkentin JD, Lin Q, Duncan SA, Olson EN (1997) Requirement of the transcription factor GATA4 for heart tube formation and ventral morphogenesis. *Genes Dev* 11(8): 1061–1072.
44. Hoffmann AD, et al. (2014) Foxf genes integrate tbx5 and hedgehog pathways in the second heart field for cardiac septation. *PLoS Genet* 10(10):e1004604.
45. Schwartz RJ, Olson EN (1999) Building the heart piece by piece: Modularity of cis-elements regulating Nkx2-5 transcription. *Development* 126(19):4187–4192.
46. Bruneau BG (2003) The developing heart and congenital heart defects: A make or break situation. *Clin Genet* 63(4):252–261.
47. Bruneau BG, et al. (1999) Chamber-specific cardiac expression of Tbx5 and heart defects in Holt-Oram syndrome. *Dev Biol* 211(1):100–108.
48. Lakso M, et al. (1996) Efficient in vivo manipulation of mouse genomic sequences at the zygote stage. *Proc Natl Acad Sci USA* 93(12):5860–5865.
49. Jiao K, et al. (2003) An essential role of Bmp4 in the atrioventricular septation of the mouse heart. *Genes Dev* 17(19):2362–2367.
50. Kisanuki YY, et al. (2001) Tie2-Cre transgenic mice: A new model for endothelial cell-lineage analysis in vivo. *Dev Biol* 230(2):230–242.
51. Joyner AL, Zervas M (2006) Genetic inducible fate mapping in mouse: Establishing genetic lineages and defining genetic neuroanatomy in the nervous system. *Dev Dyn* 235(9):2376–2385.
52. Crosio C, et al. (2002) Mitotic phosphorylation of histone H3: Spatio-temporal regulation by mammalian Aurora kinases. *Mol Cell Biol* 22(3):874–885.
53. Stambolic V, et al. (1998) Negative regulation of PKB/Akt-dependent cell survival by the tumor suppressor PTEN. *Cell* 95(1):29–39.
54. Songyang Z, Baltimore D, Cantley LC, Kaplan DR, Franke TF (1997) Interleukin 3-dependent survival by the Akt protein kinase. *Proc Natl Acad Sci USA* 94(21): 11345–11350.
55. Diao L, Chen YG (2007) PTEN, a general negative regulator of cyclin D expression. *Cell Res* 17(4):291–292.
56. Di Cristofano A, Pandolfi PP (2000) The multiple roles of PTEN in tumor suppression. *Cell* 100(4):387–390.
57. Huang W, Chang HY, Fei T, Wu H, Chen YG (2007) GSK3 beta mediates suppression of cyclin D2 expression by tumor suppressor PTEN. *Oncogene* 26(17):2471–2482.
58. He A, et al. (2014) Dynamic GATA4 enhancers shape the chromatin landscape central to heart development and disease. *Nat Commun* 5:4907.
59. He A, Kong SW, Ma Q, Pu WT (2011) Co-occupancy by multiple cardiac transcription factors identifies transcriptional enhancers active in heart. *Proc Natl Acad Sci USA* 108(14):5632–5637.
60. Mao J, et al. (2006) A novel somatic mouse model to survey tumorigenic potential applied to the Hedgehog pathway. *Cancer Res* 66(20):10171–10178.
61. Briggs LE, Kakarla J, Wessels A (2012) The pathogenesis of atrial and atrioventricular septal defects with special emphasis on the role of the dorsal mesenchymal protrusion. *Differentiation* 84(1):117–130.
62. Tian Y, et al. (2010) Characterization and in vivo pharmacological rescue of a Wnt2-Gata6 pathway required for cardiac inflow tract development. *Dev Cell* 18(2): 275–287.
63. Nadeau M, et al. (2010) An endocardial pathway involving Tbx5, Gata4, and Nos3 required for atrial septum formation. *Proc Natl Acad Sci USA* 107(45):19356–19361.
64. Yamak A, Latinkic BV, Dali R, Temsah R, Nemer M (2014) Cyclin D2 is a GATA4 co-factor in cardiogenesis. *Proc Natl Acad Sci USA* 111(4):1415–1420.
65. Luna-Zurita L, et al. (2016) Complex interdependence regulates heterotypic transcription factor distribution and coordinates cardiogenesis. *Cell* 164(5):999–1014.
66. Ang YS, et al. (2016) Disease model of GATA4 mutation reveals transcription factor cooperativity in human cardiogenesis. *Cell* 167(7):1734–1749 e1722.
67. Nakajima K, et al. (2011) Coordinated regulation of differentiation and proliferation of embryonic cardiomyocytes by a jumonji (Jarid2)-cyclin D1 pathway. *Development* 138(9):1771–1782.
68. Verzi MP, McCulley DJ, De Val S, Dodou E, Black BL (2005) The right ventricle, outflow tract, and ventricular septum comprise a restricted expression domain within the secondary/anterior heart field. *Dev Biol* 287(1):134–145.
69. Ahn S, Joyner AL (2004) Dynamic changes in the response of cells to positive hedgehog signaling during mouse limb patterning. *Cell* 118(4):505–516.
70. Bruneau BG, et al. (2001) A murine model of Holt-Oram syndrome defines roles of the T-box transcription factor Tbx5 in cardiogenesis and disease. *Cell* 106(6):709–721.